Title	Influence of emitter position of silicon heterojunction photovoltaic solar cell modules on their potential-induced degradation behaviors
Author(s)	Yamaguchi, Seira; Yamamoto, Chizuko; Ohshita, Yoshio; Ohdaira, Keisuke; Masuda, Atsushi
Citation	Solar Energy Materials and Solar Cells, 216: 110706
Issue Date	2020-08-14
Type	Journal Article
Text version	author
URL	http://hdl.handle.net/10119/18072
Rights	Copyright (C)2020, Elsevier. Licensed under the Creative Commons Attribution-NonCommercial-NoDerivatives 4.0 International license (CC BY-NC-ND 4.0). [http://creativecommons.org/licenses/by-nc-nd/4.0/] NOTICE: This is the author's version of a work accepted for publication by Elsevier. Seira Yamaguchi, Chizuko Yamamoto, Yoshio Ohshita, Keisuke Ohdaira, Atsushi Masuda, Solar Energy Materials and Solar Cells, 216, 2020, 110706, https://doi.org/10.1016/j.solmat.2020.110716
Description	

Influence of emitter position of silicon heterojunction photovoltaic solar cell modules on their potential-induced degradation behaviors

Seira Yamaguchi[1,2,3], Chizuko Yamamoto[4], Yoshio Ohshita[2,3], Keisuke Ohdaira[1], Atsushi Masuda[4*†]

[1]*Graduate School of Advanced Science and Technology, Japan Advanced Institute of Science and Technology, Nomi, Ishikawa 923-1292, Japan*

[2]*Graduate School of Engineering, Toyota Technological Institute, Tempaku, Nagoya 468-8511, Japan*

[3]*Reserach Center for Smart Energy Technology, Toyota Technological Institute, Tempaku, Nagoya 468-8511, Japan*

[4]*Research Center for Photovoltaics, National Institute of Advanced Industrial Science and Technology, Tsukuba, Ibaraki 305-8568, Japan*

*Corresponding author
E-mail address: a-masuda@eng.niigata-u.ac.jp

[†]Present address: Graduate School of Science and Technology, Niigata University, Niigata 950-2181, Japan

Abstract

Potential-induced degradation (PID)-test results of modules fabricated from the rear- and front-emitter silicon heterojunction (SHJ) solar cells were compared to clarify the influence of the emitter position of SHJ photovoltaic (PV) cell modules on their PID behaviors. The PID tests were performed by applying a bias of -2000 V to the shorted interconnector ribbons from the front surface of the cover glass, at 85 °C. In the initial stage, both modules showed the same degradation characterized by a reduction in the short-circuit current density (J_{sc}). After the first-stage degradation, the rear-emitter SHJ PV modules exhibited subsequent degradation characterized by a significant reduction in the J_{sc} and open-circuit voltage (V_{oc}), due to the enhancement of the minority-carrier recombination in the front surface region of the n-type crystalline silicon base. The front-emitter SHJ PV modules, on the other hand, showed a reduction in the fill factor (FF), in addition to moderate reductions in J_{sc} and V_{oc}. The FF reduction of the front-emitter SHJ PV modules is considered to be caused by the enhancement of the recombination in the front surface region of the n-type crystalline-silicon base as the region corresponds to the pn junction interface of the front-emitter configuration. The moderate reductions in both J_{sc} and V_{oc} may be due to further progression of the first-stage degradation. These findings are essential for understanding the mechanism of PID in SHJ PV cell modules.

1. Introduction

Recently, there has been considerable interest in silicon heterojunction (SHJ) photovoltaic (PV) cells owing to their potential to achieve high energy-conversion efficiencies. [1–8]. The SHJ PV cells feature a high-quality n-type crystalline-silicon (c-Si) base and hydrogenated amorphous-Si (a-Si) passivation films on both sides of the base, which provide remarkably high open-circuit voltages (V_{oc}s) and thus exceptionally high power-conversion efficiencies (PCEs). For example, SHJ PV cells with contact on both sides have achieved V_{oc}s higher than 730 mV, and PCEs of around 25% [4, 5]. Additionally, for more advanced SHJ cells featuring interdigitated back-contact configurations, higher PCEs have been achieved owing to the reduced shadowing losses due to the front contact grids [6–8]. According to the International Technology Roadmap for Photovoltaic (tenth edition) [9], the market share (and thus the importance) of these types of PV cells is expected to increase continuously.

It is essential to understand the possible degradation behaviors of the SHJ PV cells to ensure reliability and long-term stability. Although these PV cells have already been commercialized and installed in currently operational PV systems, the current understanding of the possible degradation behaviors in these cells is still inadequate. Potential-induced degradation (PID) [10–13] is considered one of the most important reliability issues of PV modules as it often causes significant performance losses in a relatively short time. PID is a type of performance deterioration that is triggered by electric potential differences between the grounded frames and the cells. It is found mainly in large-scale PV systems, as the system bias in such installations is very high. PID has been reported in various types of PV modules fabricated from conventional p-type c-Si cells [11–15]; conventional n-type c-Si cells [16–20]; n-type c-Si cells with rear-side emitters [20, 21]; n-type interdigitated back contact cells [22, 23], including those with front floating emitters [24]; thin-film a-Si cells [25–27]; copper indium gallium selenide thin-film cells [28–30]; and cadmium telluride thin-film cells [27, 30, 31]. Since the degradation behavior of PV modules is known to be strongly affected by their cell and module structures, PID should be investigated for each type of PV cell or module.

There are a few reports on the PID in SHJ PV modules [32–36]. Certain groups have reported that commercial SHJ PV modules do not undergo any degradation under negative- and positive-bias stresses [32–34], thus demonstrating that they have an excellent resistance to PID. However, in our previous studies [35, 36], where rear-emitter SHJ PV cell modules with traditional, low-cost encapsulation materials were used, SHJ PV cell modules were found to undergo PID characterized mainly by the reduction in the short-circuit current density (J_{sc}). This implies that a high PID resistance is mainly due to their encapsulation materials. The J_{sc} reduction was confirmed to be due to the chemical reduction of indium oxide in the front transparent conductive oxide (TCO) films [36]. The first-stage degradation does not show a significant regeneration by applying an opposite bias [35], unlike the PID of many other types of modules. This irreversibility may be because the degradation is caused by an irreversible chemical reaction. Additionally, if the degradation proceeds further, the V_{oc} will reduce significantly, potentially due to the

enhancement of the recombination in the front a-Si/c-Si interface regions caused by sodium introduction [36]. (In this paper, these degradations are referred to as the first-stage and second-stage degradations, respectively.) However, the PID behaviors of front-emitter SHJ PV cell modules have not yet been reported.

In this paper, we clarify the influence of the emitter position of SHJ PV cell modules on their potential-induced degradation behaviors by comparing the PID-test results of rear- and front-emitter SHJ PV cell modules. For the first-stage degradation the cause is the darkening of the front TCO, and, therefore, the degradation behavior is expected to be unchanged regardless of the emitter position. To confirm this can be an indirect evidence of hypothesis for a proposed degradation mechanism in previous studies [35, 36]. However, in the second-stage degradation, rear- and front-emitters of the SHJ PV modules may show different PID behaviors. These findings improve the understanding of PID in SHJ PV modules and may contribute to improvements in the reliability and long-term stability of SHJ PV cell modules.

2. Experimental procedures

Single-cell 180×180 mm^2 SHJ PV cell modules were fabricated using 156×156-mm^2 commercial bifacial n-type SHJ solar cells with a rear-side emitter and tungsten-doped indium oxide (IWO) TCO films. Fig. 1 shows the cell structure. The modules had the following structure: a 3.2-mm-thick tempered white cover glass, a 450-μm-thick ethylene-vinyl acetate copolymer (EVA) sheet (fast cure type), the SHJ solar cell, a 450-μm-thick EVA sheet (fast cure type), and a typical white back sheet [38-μm-thick poly(vinyl fluoride) sheet, a 250-μm-thick poly(ethylene terephthalate) sheet, and a 38-μm-thick poly(vinyl fluoride) sheet]. The rear- and front-emitter modules were fabricated by laminating the cells with the emitter side down and up, respectively. Standard EVA sheets, used in this study, had a relatively low volume resistivity of 1.5×10^{14} Ω·cm and were not capable of preventing PID. The module lamination process consisted of two stages, namely, a degassing stage, lasting 5 min, and an adhesion stage, lasting 15 min. Both processes were conducted on a hot plate maintained at 135 °C.

Accelerated PID tests were performed by applying a high negative bias of −2000 V to shorted module-interconnector ribbons, relative to a grounded aluminum plate placed on the front surface of the module cover glass in a heating chamber maintained at 85 °C. When the rear- (front-) emitter modules were tested, electric fields were mainly formed between the glass surface and n (p) side. Herein, the term "negative bias" indicates a bias that produces cells with negative potentials with respect to the aluminum plate. We used such a high negative bias as it is known to improve the repeatability of the PID tests significantly [35, 36]. The relative humidity in the heating chamber was very low (<2% RH). Note that humidity (and resulting moisture ingress) influences the degradation, which is significantly accelerated under humid conditions [37]. We performed one-sun-illuminated and dark current density–voltage (J–V) measurements, and external quantum efficiency (EQE) measurements on the modules before and after the PID tests to evaluate the degradation.

4

3. Results

One-sun-illuminated J–V measurements were taken at the rear- and front-emitter SHJ PV cell modules before and after the PID tests to clarify the influence of the emitter position. Fig. 2 shows the representative one-sun-illuminated J–V characteristics of the SHJ PV cell modules before and after the PID tests with a negative bias of -2000 V, for 30 and 72 days, at 85 °C. With regard to the initial PV cell performance, the front-emitter SHJ PV cell module shows a lower J_{sc} than that of the rear-emitter module. This is mainly caused by a difference in the areas of the front surface grid electrodes. Both modules exhibit the first-stage degradation characterized by reductions in the J_{sc} within 30 days. However, different behaviors were observed in the second-stage degradation.

The rear-emitter SHJ PV cell module shows an even larger reduction in J_{sc} and V_{oc}, which are the same as reported previously. However, the reductions in the J_{sc} and V_{oc} in the front-emitter SHJ PV cell module were considerably smaller than those observed in the rear-emitter module. The front-emitter SHJ PV cell module shows a moderately reduced fill factor (FF), which is not observed in the PID in the rear-emitter module. Fig. 3 shows the detailed PID-stress-duration dependence of the normalized J_{sc}, V_{oc}, FF, and maximum output power (P_{max}), where $J_{sc,0}$, $V_{oc,0}$, FF_0, and $P_{max,0}$ are the initial J_{sc}, V_{oc}, FF, and P_{max}, respectively. For both types of modules, the J_{sc} decreases at almost the same degradation rate until the PID-stress duration reaches 30 days. No differences were observed in the behavior in the first-stage degradation. However, differences were observed in the behaviors of the two kinds of modules in the second-stage degradation (observed beyond the 30-day mark). The J_{sc} reduction of the rear-emitter SHJ PV cell modules is significantly accelerated and is accompanied by a substantial reduction in the V_{oc}. Contrarily, the rate of reduction of the J_{sc} of the front-emitter modules is maintained even after 30 days, and no significant V_{oc} reduction is observed. Additionally, the FF increases for the rear-emitter SHJ PV modules, whereas it reduces for the front-emitter modules. As a result of the above differences, the rear-emitter SHJ PV cell modules showed more significant degradation in the P_{max}.

Dark J–V measurements were also performed to observe changes in the diode characteristics. Fig. 4 shows the representative dark J–V characteristics of the rear- and front-emitter SHJ PV cell modules, before and after the PID tests in which a negative bias of -2000 V was applied for 30 and 72 days. The first-stage degradation has been reported to be caused by the darkening of the front IWO films [36]. Therefore, the first-stage degradation cannot be observed as changes in the dark J–V characteristics. After the 72-day PID test, the rear-emitter SHJ PV cell modules showed a significant increase in the diffusion currents ($V \geq 0.35$ V), implying enhancement in the bulk and/or interface recombination. This can be considered as the beginning of the second-stage degradation, characterized by reductions in the J_{sc} and V_{oc}. In contrast, the front-emitter SHJ PV cell modules do not show an enhancement in the diffusion currents, and instead, exhibit an increase in recombination currents ($V \leq 0.35$ V), implying an enhancement in the recombination between majority carriers that diffuse into the interface depletion region, from both sides of the pn junction.

The representative EQE spectra of the rear- and front-emitter SHJ PV cell

modules, before and after the PID tests with a negative bias of -2000 V for 30 and 72 days, are shown in Fig. 5. Both modules show a reduction in the EQE over the entire wavelength range after the PID tests for 30 days. This corresponds with the first-stage degradation, characterized by a reduction in J_{sc}. The EQE reduction is reported to be mainly caused by the darkening of the front TCO films [36]. After the PID tests for 72 days, the rear-emitter SHJ PV cell module shows a further reduction in the EQE over the entire wavelength range, particularly in the short-wavelength range. This indicates a potential enhancement in the interface and/or bulk recombination in the vicinity of the front surface of the n-type c-Si base. In contrast, the front-emitter SHJ PV cell module shows no significant reduction in the EQE.

4. Discussion

As shown in Figs. 2a and 3, the rear-emitter PV modules showed the first-stage degradation, characterized by a reduction in the J_{sc}, and the second-stage degradation, characterized by an additional reduction in the J_{sc} and a decrease in the V_{oc}. In contrast, the front-emitter SHJ PV cell modules exhibited the first-stage degradation behavior similar to that observed in the rear-emitter modules, and, however, it underwent a different second-stage degradation, characterized by moderate reductions in J_{sc}, V_{oc}, and FF (Fig. 2b and Fig. 3). This indicates that the rear- and front-emitters SHJ PV cell modules undergo the same first-stage degradation but show different behaviors in the second-stage of degradation.

In the first-stage degradation, the same degradation occurs in both the rear- and front-emitter SHJ PV cell modules as they have the same kind of front TCO layers. The origin of the first-stage degradation has been identified as the darkening of the front TCO, caused by the precipitation of metal indium resulting from the chemical reduction of indium oxides [36]. Both modules have the same IWO TCO, and the same chemical reduction reaction should occur in both modules.

In contrast, the emitter position impacts the behavior of the second-stage degradation of the rear- and front-emitter PV cell modules. The second-stage degradation has been reported to be triggered by the enhancement of the bulk/interface recombination caused by the formation of defect levels with sodium introduction into the front surface region of the n-type base and/or damage to the front a-Si passivation layer [36]. Thus, the defect levels in the vicinity of the front side of the c-Si base are introduced regardless of the emitter position. In the rear-emitter SHJ PV cells, the front surface region is far from the pn junction interface. The introduced defect levels cause the recombination of the photo-generated excess carriers and the enhancement of the diffusion currents of the pn junction, leading to reductions in J_{sc} and V_{oc}, respectively. This is consistent with the results of the dark J–V characteristics, shown in Fig. 4a, and the EQE spectra. In Fig. 4a, an increase in the diffusion current is observed. The EQE, as shown in Fig. 5a, exhibited a reduction in the EQE in the short-wavelength range, implying an enhancement in the photo-generated carrier recombination in the vicinity of the surface region of the n-type c-Si base. However, the front-surface region of the n-type c-Si base corresponds to the pn junction interface region for the front-emitter SHJ PV cells. Therefore, if defect levels are introduced there, diffusion currents do not increase

6

and do not lead to reductions in the J_{sc} and V_{oc}. (Moderate reductions in the J_{sc} and V_{oc} were observed potentially caused by the progression of the first-stage degradation. The V_{oc} reduction is due to the reduction in the J_{sc}, namely, the decrease in the photo-generated excess carriers.) Instead, recombination in the pn junction interface is enhanced, which may, in turn, enhance the recombination currents and, therefore, decrease the FF. (Here, "recombination currents" refers to currents via the recombination between majority carriers from both sides of the pn junction.)

From the perspective of large-scale PV system installations, front-emitter SHJ PV cell modules may be superior to rear-emitter modules owing to the considerably lower second-stage degradation in front-emitter SHJ PV cell modules. The type of PV cell module to be used should be determined after considering the initial performance. The findings obtained in this study will, however, be useful in selecting PV cell modules used in large-scale PV systems.

The acceleration factor should also be considered from the perspective of the field relevance. However, it is difficult to discuss the acceleration factor of this test because of the lack of findings of the field degradation. In this study, to observe the second-stage degradation, a high negative bias of -2000 V was applied to the modules for a relatively long time. The condition is severe compared to the standard PID test conditions. However, the absence of second-stage degradation in the field cannot be predicted. In this study, the relative humidity was <2%. We have reported that SHJ PV modules pre-stressed in a conventional damp heat test for 700 h showed approximately 20-times faster PID [37], implying that the SHJ modules stressed in a humid environment are more easily degraded by PID stress. There are open questions related to the field relevance, including the acceleration factor. Additional work is required to discuss the on-ground relevance of this study in detail.

5. Conclusions

We investigated the influence of the emitter position on the PID behaviors of SHJ PV cell modules by comparing the results of the rapid PID tests of the rear- and front-emitter modules.

We found that the SHJ PV cell modules show the same first-stage degradation, characterized by a reduction in the J_{sc}, regardless of the emitter position. This degradation is known to be caused by the darkening of the front TCO layer. Both the rear- and front-emitter SHJ PV modules had the same IWO TCO in the front, resulting in a similar degradation.

In the second-stage degradation, the rear-emitter SHJ PV cell modules showed a degradation characterized by significant reductions in both the J_{sc} and V_{oc}. Based on the dark J–V and EQE characteristics, we found that the degradation was due to an enhancement in the bulk/interface recombination in the vicinity of the front surface of the n-type c-Si base. However, the front-emitter SHJ PV modules showed a moderate reduction in the FF, potentially caused by the enhanced recombination at the pn junction interface. This difference in the second-stage degradation may be because the surface region of the n-type c-Si base in the rear-emitter cells is far from the pn junction interface, whereas that of the base in the front-emitter cells

corresponds to the pn junction interface. The front-emitter modules also showed moderate reductions in the J_{sc} and V_{oc}. However, these reductions were due to the progression of the first-stage degradation. As a result of the second-stage degradation, the rear-emitter SHJ PV cell modules exhibited a larger performance deterioration than that in front-emitter SHJ PV cell modules.

These findings improve the understanding of PID in SHJ PV cell modules and may contribute to improvements in their reliability and long-term stability.

Acknowledgments

References

[1] S. de Wolf, A. Descoeudres, Z.C. Holman, C. Ballif, High-efficiency silicon heterojunction solar cells: A review, Green **2** (2012) 7–24.

[2] T. Mishima, M. Taguchi, H. Sakata, E. Maruyama, Development status of high-efficiency HIT solar cells, Sol. Energy Mater. Sol. Cells **95** (2011) 18–21.

[3] T. Kinoshita, D. Fujishima, A. Yano, A. Ogane, S. Tohoda, K. Matsuyama, Y. Nakamura, N. Tokuoka, H. Kanno, H. Sakata, M. Taguchi, E. Maruyama, The approaches for high efficiency HIT solar cell with very thin (<100 μm) silicon wafer over 23%, In: Proceedings of the 26th European Photovoltaic Solar Energy Conference and Exhibition, 2011, pp. 871– 874.

[4] M. Taguchi, A. Yano, S. Tohoda, K. Matsuyama, Y. Nakamura, T. Nishiwaki, K. Fujita, E. Maruyama, 24.7% record efficiency HIT solar cell on thin silicon wafer, IEEE J. Photovolt. **4** (2014) 96–99.

[5] D. Adachi, J.L. Hernández, K. Yamamoto, Impact of carrier recombination on fill factor for large area heterojunction crystalline silicon solar cell with 25.1% efficiency, Appl. Phys. Lett. **107** (2015) 233506.

[6] K. Masuko, M. Shigematsu, T. Hashiguchi, D. Fujishima, M. Kai, N. Yoshimura, T. Yamaguchi, Y. Ichihashi, T. Mishima, N. Matsubara, T. Yamanishi, T. Takahama, M. Taguchi, E. Maruyama, S. Okamoto, Achievement of more than 25% conversion efficiency with crystalline silicon heterojunction solar cell, IEEE J. Photovolt. **4** (2014) 1433–1435.

[7] K. Yoshikawa, H. Kawasaki, W. Yoshida, T. Irie, K. Konishi, K. Nakano, T. Uto, D. Adachi, M. Kanematsu, H. Uzu, K. Yamamoto, Silicon heterojunction solar cell with interdigitated back contacts for a photoconversion efficiency over 26%, Nat. Energy **2** (2017) 17032.

[8] K. Yamamoto, K. Yoshikawa, H. Uzu, D. Adachi, High-efficiency heterojunction crystalline Si solar cells, Jpn. J. Appl. Phys. **57** (2018) 08RB20.

[9] SEMI PV Group Europe. International Technology Roadmap for Photovoltaic (ITRPV), 2018 Results, https://itrpv.vdma.org, 2019 (accessed 06.11.19).

[10] W. Luo, Y.S. Khoo, P. Hacke, V. Naumann, D. Lausch, S.P. Harvey, J.P. Singh, J. Chai, Y. Wang, A.G. Aberle, S. Ramakrishna, Potential-induced degradation in photovoltaic modules: a critical review, Energy Environ. Sci. **10** (2017) 43–68.

[11] S. Pingel, O. Frank, M. Winkler, S. Daryan, T. Geipel, H. Hoehne, J. Berghold, Potential induced degradation of solar cells and panels, In: Proceedings of the 35th IEEE Photovoltaic Specialists Conference, 2010, pp. 2817–2822.

[12] J. Berghold, O. Frank, H. Hoehne, S. Pingel, S. Richardson, M. Winkler, Potential induced degradation of solar cells and panels, In: Proceedings of the 25th European Photovoltaic Solar Energy Conference and Exhibition/5th World Conference on Photovoltaic Energy Conversion, 2010, pp. 3753–3759.

[13] P. Hacke, M. Kempe, K. Terwilliger, S. Glick, N. Call, S. Johnston, S. Kurtz, I. Bennett, M. Kloos, Characterization of multicrystalline silicon modules with system bias voltage applied in damp heat, In: Proceedings of the 25th European Photovoltaic Solar Energy Conference and Exhibition/5th World Conference on Photovoltaic Energy Conversion, 2010, pp. 3760–3765.

[14] V. Naumann, D. Lausch, A. Graff, M. Werner, B. Swatek, J. Bauer, A. Hähnel,

O. Breitenstein, S. Großer, J. Bagdahn, C. Hagendorf, The role of stacking faults for the formation of shunts during potential-induced degradation of crystalline Si solar cells, Phys. Status Solidi: Rapid Res. Lett. **7** (2013) 315–318.

[15] V. Naumann, D. Lausch, A. Hähnel, J. Bauer, O. Breitenstein, A. Graff, M. Werner, S. Swatek, S. Großer, J. Bagdahn, C. Hagendorf, Explanation of potential-induced degradation of the shunting type by Na decoration of stacking faults in Si solar cells, Sol. Energy Mater. Sol. Cells **120** (2014) 383–389.

[16] K. Hara, S. Jonai, A. Masuda, Potential-induced degradation in photovoltaic modules based on n-type single crystalline Si solar cells, Sol. Energy Mater. Sol. Cells **140** (2015) 361–365.

[17] S. Yamaguchi, A. Masuda, K. Ohdaira, Progression of rapid potential-induced degradation of n-type single-crystalline silicon photovoltaic modules, Appl. Phys. Express **9** (2016) 112301.

[18] S. Bae, W. Oh, K.D. Lee, S. Kim, H. Kim, N. Park, S.-I. Chan, S. Park, Y. Kang, H.-S. Lee, D. Kim, Potential induced degradation of n-type crystalline silicon solar cells with p$^+$ front junction, Energy Sci. Eng. **5** (2017) 30–37.

[19] K. Hara, K. Ogawa, Y. Okabayashi, H. Matsuzaki, A. Masuda, Influence of surface structure of n-type single-crystalline Si solar cells on potential-induced degradation, Sol. Energy Mater. Sol. Cells **166** (2017) 132–139.

[20] M. Barbato, A. Barbato, M. Meneghini, G. Tavernaro, M. Rossetto, G. Meneghesso, Potential induced degradation of N-type bifacial silicon solar cells: An investigation based on electrical and optical measurements, Sol. Energy Mater. Sol. Cells **168** (2017) 51–61.

[21] S. Yamaguchi, A. Masuda, K. Ohdaira, Changes in the current density-voltage and external quantum efficiency characteristics of n-type single-crystalline silicon photovoltaic modules with a rear-side emitter undergoing potential-induced degradation, Sol. Energy Mater. Sol. Cells **151** (2016) 113–119.

[22] R. Swanson, M. Cudzinovic, D. DeCeuster, V. Desai, J. Jürgens, N. Kaminar, W. Mulligan, L. Rodrigues-Barbosa, D. Rose, D. Smith, A. Terao, K. Wilson, The surface polarization effect in high-efficiency silicon solar cells. In: Technical Digest of the 15th International Photovoltaic Science and Engineering Conference, 2005, pp. 410–411.

[23] V. Naumann, T. Geppert, S. Großer, D. Wichmann, H.-J. Krokoszinski, M. Werner, C. Hagendorf, Potential-induced degradation at interdigitated back contact solar cells, Energy Procedia **55** (2014) 498–503.

[24] A. Halm, A. Schneider, V.D. Mihailetchi, L.J. Koduvelikulathu, L.M. Popescu, G. Galbiati, H. Chu, R. Kopecek, Potential-induced degradation for encapsulated n-type IBC solar cells with front floating emitter. Energy Procedia **77** (2015) 356–363.

[25] C.R. Osterwald, T.J. McMahon, J.A. del Cueto, Electrochemical corrosion of SnO$_2$: F transparent conducting layers in thin-film photovoltaic modules. Sol. Energy Mater. Sol. Cells **79** (2003) 21–33.

[26] A. Masuda, Y. Hara, Potential-induced degradation of thin-film Si photovoltaic modules, Jpn. J. Appl. Phys **56** (2017) 04CS04.

[27] A. Masuda, Y. Hara, Y. Shiina, S. Okamoto, T. Okamoto, Similarity of potential-induced degradation in superstrate-type thin-film CdTe and Si photovoltaic modules, Jpn. J. Appl. Phys. **58** (2019) SBBF07.

[28] V. Fjällström, P.M.P. Salomé, A. Hultqvist, M. Edoff, T. Jarmar, B.G. Aitken, K. Zhang, K. Fuller, C.K. Williams, Potential-induced degradation of $CuIn_{1-x}Ga_xSe_2$ thin film solar cells, IEEE J. Photovolt. **3** (2013) 1090–1094.

[29] S. Yamaguchi, S. Jonai, K. Hara, H. Komaki, Y. Shimizu-Kamikawa, H. Shibata, S. Niki, Y. Kawakami, A. Masuda, Potential-induced degradation of $Cu(In,Ga)Se_2$ photovoltaic modules, Jpn. J. Appl. Phys. **54** (2015) 08KC13.

[30] P. Hacke, K. Terwilliger, S.H. Glick, G. Perrin, J. Wohlgemuth, S. Kurtz, K. Showalter, J. Sherwin, E. Schneller, S. Barkaszi, R. Smith, Survey of potential-induced degradation in thin-film modules, J. Photon. Energy **5** (2015) 053083.

[31] P. Hacke, S. Spataru, S. Johnston, K. Terwilliger, K. VanSant, M. Kempe, J. Wohlgemuth, S. Kurtz, A. Olsson, M. Propst, Elucidating PID degradation mechanisms and in situ dark I–V monitoring for modeling degradation rate in CdTe thin-film modules, IEEE J. Photovolt. **6** (2016) 1635–1640.

[32] Z. Xiong, T.M. Walsh, A.G. Aberle, PV module durability testing under high voltage biased damp heat conditions, Energy Procedia **8** (2011) 384–389.

[33] T. Ishiguro, H. Kanno, M. Taguchi, S. Okamoto, Study on PID resistance of HIT PV modules, presented at 2013 Photovoltaic Module Reliability Workshop, 2013.

[34] N. Riedel, L. Pratt, E. Moss, M. Yamasaki, 600 hour potential induced degradation (PID) testing on silicon, CIGS, and HIT modules, presented at 2015 NREL Photovoltaic Module Reliability Workshops, 2015.

[35] S. Yamaguchi, C. Yamamoto, K. Ohdaira, A. Masuda, Reduction in the short-circuit current density of silicon heterojunction photovoltaic modules subjected to potential-induced degradation tests, Sol. Energy Mater. Sol. Cells **161** (2017) 439–443.

[36] S. Yamaguchi, C. Yamamoto, K. Ohdaira, A. Masuda, Comprehensive study of potential-induced degradation in silicon heterojunction photovoltaic cell modules, Prog. Photovolt.: Res. Appl. **26** (2018) 697–708.

[37] A. Masuda, C. Yamamoto, Y. Hara, S. Jonai, Y. Tachibana, T. Toyoda, T. Minamikawa, S. Yamaguchi, K. Ohdaira, Influence of hygrothermal stress on potential-induced degradation for homojunction and heterojunction crystalline Si photovoltaic modules, Jpn. J. Appl. Phys. (in press) [DOI: 10.35848/1347-4065/ab9a8a].

Figure captions

Figure 1. Schematic diagram of the structure of the bifacial SHJ PV cells used in this study.

Figure 2. Representative one-sun-illuminated J–V characteristics of (a) rear- and (b) front-emitter SHJ PV cell modules before and after the PID tests for 30 and 72 days.

Figure 3. (a) $J_{sc}/J_{sc,0}$, (b) $V_{oc}/V_{oc,0}$, (c) FF/FF_0, and (d) $P_{max}/P_{max,0}$ as a function of PID-stress duration. The data points represent the mean values of two identical modules. The solid and dashed lines are visual guides.

Figure 4. Representative dark J–V characteristics of (a) rear- and (b) front-emitter SHJ PV cell modules before and after the PID tests for 30 and 72 days.

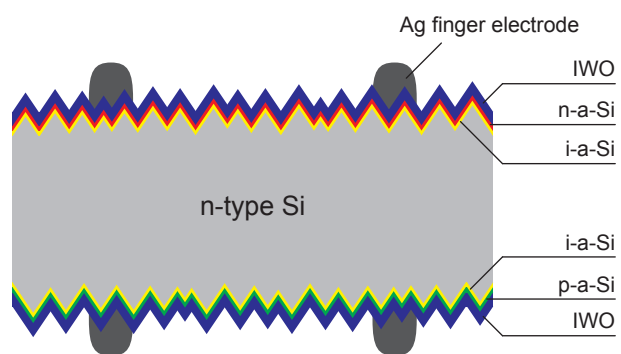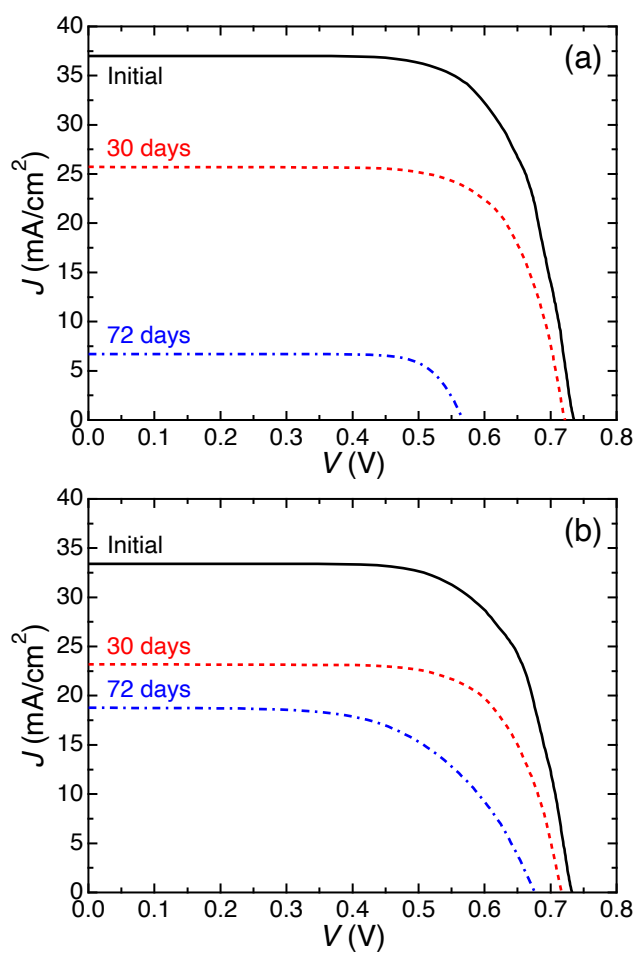**Figure 5.** Representative EQE spectra of (a) rear- and (b) front-emitter SHJ PV cell modules before and after the PID tests for 30 and 72 days.
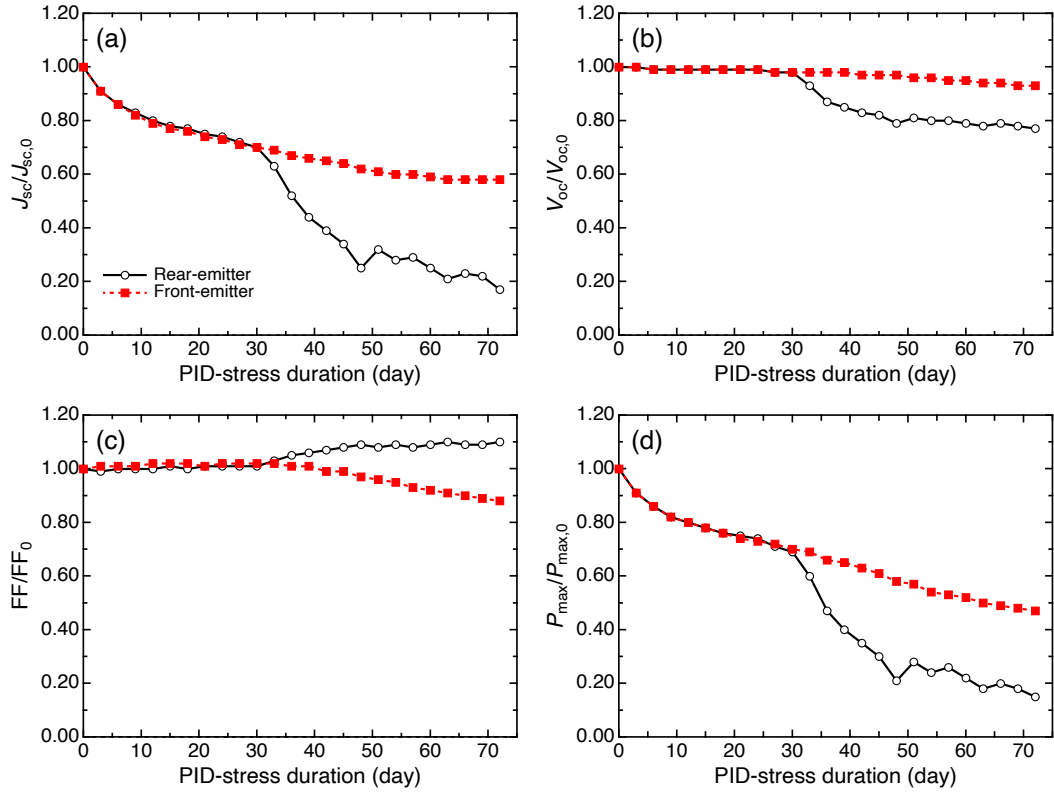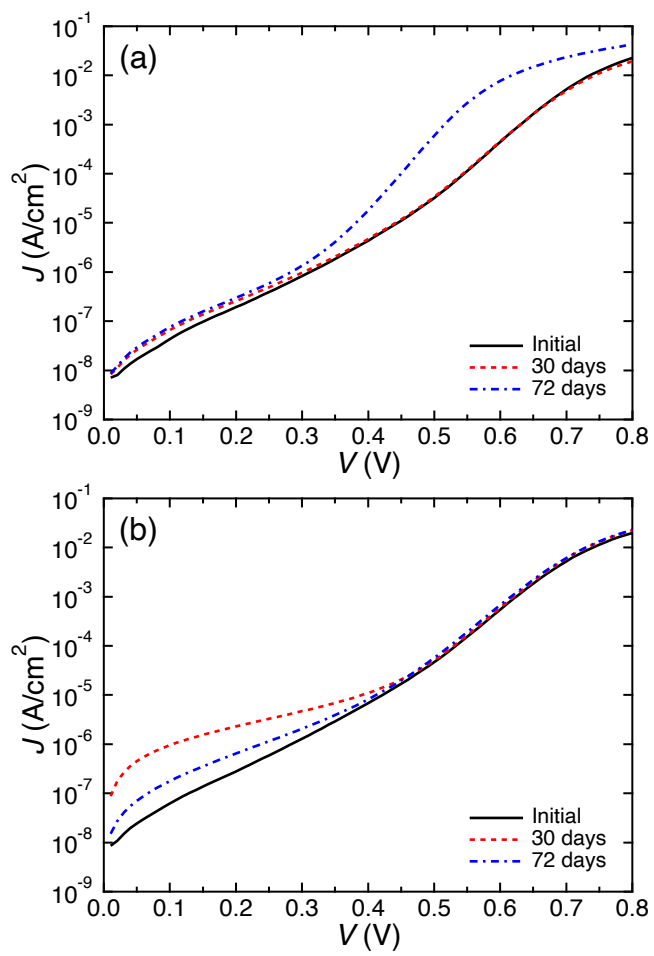
Fig. 1

Fig. 2

Fig. 3

Fig. 4

Fig. 5